

## Physicochemical Study and Corrosion Inhibition Potential of *Ficus tricopoda* for Aluminium in Acidic Medium

N.O. Eddy,<sup>a,b,\*</sup> P.O. Ameh,<sup>a</sup> M.Y. Gwarzo,<sup>a</sup> I.J. Okop<sup>b</sup> and S.N. Dodo<sup>a</sup>

<sup>a</sup> Department of Chemistry, Ahmadu Bello University, Zaria, Kaduna State, Nigeria

<sup>b</sup> Department of Chemistry, Akwa Ibom State University, Ikot Akpaeden. Mkpata Enin, Akwa Ibom State, Nigeria

Received 24 November 2012; accepted 23 April 2013

---

### Abstract

Gas chromatography mass spectrophotometer (GCMS) analysis of *Ficus tricopoda* gum indicated the presence of 4.75, 56.15, 32.10 and 7.00 % of camphene, sucrose, 2-methylene cholestan-3-ol and 7-hexadecenal, respectively. Several stretching and bending vibrations were observed in the Fourier transformed infra-red (FTIR) spectrum of the gum. Physicochemical examinations of the gum revealed that it is pale yellow in colour, mildly acidic, ionic and display characteristics of sour taste. The solubility of the gum in water was found to increase with increase in temperature. Knowledge of the chemical constitution of the gum (hence chemical structures of its constituents) was useful in predicting the corrosion inhibition potential of *Ficus tricopoda* (FT) gum. Consequently, the gum was found to be a good adsorption inhibitor for the corrosion of aluminum in solution of H<sub>2</sub>SO<sub>4</sub>. The adsorption of the gum (which, followed first order kinetic) was found to be endothermic at FT gum critical concentration of 0.3 g/L and exothermic at concentrations above the critical limit. The short coming of the Langmuir adsorption model in describing the existent of interaction between the molecules of the gum was complimented by the Frumkin and Dubinin-Radushkevich adsorption models. Calculated values of activation and free energies of activation indicated that the adsorption of *Ficus tricopoda* gum on Al surface exhibited both physical and chemical adsorption mechanism.

**Keywords:** corrosion, aluminum, inhibition, *Ficus tricopoda* gum.

---

### Introduction

Corrosion inhibition is essential in combating the negative environmental and industrial impact of corrosion; being one of the most effective methods of

---

\* Corresponding author. E-mail nabukeddy@yahoo.com

preventing metal in petroleum, fertilizers, metallurgical and other industries, corrosion inhibition is concern with the use of chemical substances that can retard the rate of corrosion of a metal in contact with an aggressive medium [1-2].

Several researches have been successful in the discovery of broad ranges of inhibitors for the control of corrosion [3-5]. However, current challenges are based on utilization of inhibitors that are environmentally friendly, easy available, cost effective and biodegradable [6]. These conditions are hardly fulfilled by most inorganic inhibitors such as chromate and heavy metal rich compounds, hence current researches are directed towards the use of green inhibitors for the inhibition of the corrosion of metals [7-9]. On the list there are extracts of plant and animal and some gum exudates [10-17].

Available literature revealed that most corrosion inhibitors are chosen through knowledge of their chemical structures [18]. Generally, organic compounds that contain either hetero atoms, aromatic ring,  $\pi$ -electron, or long carbon chain are found to be effective corrosion inhibitors [19]. Therefore, the present study is aimed at investigating the physicochemical parameters of FT gum and its potential as a green inhibitor for the corrosion of aluminum in HCl medium.

### **Materials and methods**

Samples of *Ficus tricopoda* (FT) gum were obtained as dried exudates from their parent trees grown at Samaru, Zaria in Sabon Gari LGA of Kaduna State of Nigeria. The outer bark of the tree was broken using a small axe. The cut was widened upward and downward and the gum formed was collected. The crude gum was purified through dissolution in cold distilled water. The solution was strained through muslin and centrifuged to obtain a small quantity of a dense gel. The straw coloured supernatant liquor obtained was separated and acidified to a pH of 2 with dilute hydrochloric acid. Ethyl alcohol was added until the liquor was 80 percent alcohol. The gum precipitated out was removed by centrifugation at a rate of 2000 revolution per minutes, washed with alcohol, ether and dried in a desiccator [20].

### ***Determination of physicochemical properties of the gum***

The pH of the gum was determined using a pre calibrated Oklon pH meter. The solubility of the gum was determined in cooled and hot distilled water, acetone and chloroform using the method reported by Carter [21].

### ***Corrosion studies***

Aluminum alloy sheet of composition (wt. %, as determined by quantimetric method) Mn (1.28), Pb (0.064), Zn (0.006), Ti (0.029), Cu (0.81), Si (0.381), Fe (0.57) and Al (96.65%) was used. The sheets were mechanically pressed and cut into different coupons, each of dimensions, 5 x 4 x 0.11cm. Each coupon was degreased by washing with ethanol, cleaned with acetone and allowed to dry in the air before preservation in a desiccator. All reagents used for the study were analar grade and double distilled water was used for their preparation.

Weight loss and hydrogen evolution experiments were carried out as reported elsewhere [18]. From weight loss measurements, inhibition efficiency, corrosion rate and degree of surface coverage were calculated using the following equations

$$\%I = \left(1 - \frac{W_1}{W_2}\right) \times 100 \quad (1)$$

$$\theta = \left(1 - \frac{W_1}{W_2}\right) \quad (2)$$

$$CR = \frac{\Delta W}{At} \quad (3)$$

where  $W_1$  and  $W_2$  are the weight losses (g) for aluminum in the presence and absence of the inhibitor,  $\theta$  is the degree of surface coverage of the inhibitor,  $\Delta W = W_2 - W_1$ ,  $A$  is the area of the aluminum coupon (in  $\text{cm}^2$ ),  $t$  is the period of immersion (in hours) and  $\Delta W$  is the weight loss of aluminum after time,  $t$ . In gasometric experiment, the test solution was poured into the reaction vessel. Upon the introduction of mild steel, the flask was quickly corked and the rise in volume of the paraffin due to hydrogen evolution was noted after every minute until a steady volume was observed. Inhibition efficiency was calculated as the quotient of the difference between the volume of hydrogen evolved by the blank and that of the test solution to the volume of hydrogen evolved by the blank.

#### ***FTIR analysis***

FTIR analysis of the gum was carried out and that of the corrosion products (in the absence and presence of the gum) were carried out using a Scimadzu FTIR-8400S Fourier transform infra-red spectrophotometer. The sample was prepared in KBr and the analysis was carried out by scanning the sample through a wave number range of 400 to 4000  $\text{cm}^{-1}$ .

#### ***GC-MS analysis***

GC-MS analysis was carried out on a GC Clarus 500 Perkin Elmer system comprising of an AOC-20i auto-sampler and gas chromatograph interfaced to a mass spectrometer (GC-MS) instrument employing the following conditions: column Elite-1 fused silica capillary column (30 x 0.25 mm ID x 1  $\mu\text{M}$  df, composed of 100 % dimethylpoly diloxane), operating in electron impact mode at 70 eV; helium (99.999 %) was used as carrier gas at a constant flow of 1 mL/min and an injection volume of 0.5  $\mu\text{L}$  was employed (split ratio of 10:1) at an injector temperature of 250  $^\circ\text{C}$ ; ion-source temperature of 280  $^\circ\text{C}$ . The oven temperature was programmed from 110  $^\circ\text{C}$  (isothermal for 2 min), with an increase of 10  $^\circ\text{C}/\text{min}$ , to 200  $^\circ\text{C}$ , then 5  $^\circ\text{C}/\text{min}$  to 280  $^\circ\text{C}$ , ending with a 9 min isothermal at 280  $^\circ\text{C}$ . Mass spectra were taken at 70 eV; a scan interval of 0.5 seconds and fragments from 40 to 450 Da. Total GC running time was 36 min.

Interpretation on mass spectrum GC-MS was conducted using the database of the National Institute Standard and Technology (NIST) Abuja, having more than

62,000 patterns. The spectrum of the unknown component was compared with the spectra of the known components stored in the NIST library. The name, molecular weight and structure of the components of the test materials were ascertained. The concentrations of the identified compounds were determined through area and height normalization.

**Table 1.** Physicochemical properties of *FT* gum.

Parameters	Property
Color	Pale- yellow
Odour	Sweet
Taste	Sour taste
pH	4.10
Percentage yield (% w/w)	72.00
Solubility (% w/v)	
(i) Cold water	14.20
(ii) Hot water	15.10
(iii) Acetone	0.00
(iv) Chloroform	0.00
(v) Ethanol	0.40

## Results and discussions

### *Physiochemical parameters of FT gum*

Table 1 presents the physiochemical parameters of *FT* gum including colour, pH, percentage yield and solubility in various solvents. The gum is pale yellow in colour (Fig.1), it has a sour taste and a sweeten odor. The measured pH of the gum (4.10) revealed that the gum is acidic and is characterized with a sour taste. The solubility of the *FT* gum in water tends to increase with increase in temperature, indicating that the heat given off in dissolving the gum is less than the heat required to break the gum apart. The net dissolution reaction is endothermic (energy required). Therefore, addition of more heat facilitates the dissolution of the gum by providing energy to break bonds within the gums. The gum was also found to be slightly soluble in ethanol but insoluble in acetone and chloroform. The solubility of the gum in ethanol may be due to the presence of polar and non-polar ends in ethanol, which made it to dissolve some polar and non-polar compounds. On the other hand, chloroform and acetone are non-polar solvents and as expected, non-polar compounds are soluble in non-polar solvent and vice versa. Hence *FT* gum is ionic and it is expected to be insoluble in chloroform and acetone.

### *GCMS study of FT gum*

Fig. 2 shows the GCMS spectrum of *FT* gum. From the figure it can be seen that the spectrum of *FT* gum is characterized with four peaks. Since the area under the GCMS peak is proportional to the concentration, results obtained from area normalization were used to estimate the percentage concentrations of identified constituents of the gum, as presented in Table 2. The table also presents the various fragmentation peaks associated with each of the fraction, the

corresponding retention time, molar mass and chemical formula of the identified compounds. In Fig. 3, chemical structures of the identified compounds are displayed. The numbering on each of the structures corresponds to the peak number in the spectrum (Fig.2). The results obtained indicated that major components of FT gum are sucrose (56.15 %) and 2-methylene-3-ol (32.10 %), while camphene (4.75 %) and 7-hexadecenal (7.00 %) are its minor components.



Figure 1. Samples of unprocessed and processed FT gum.

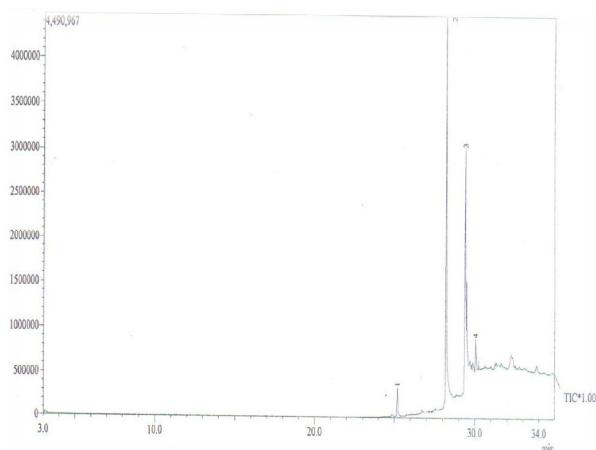
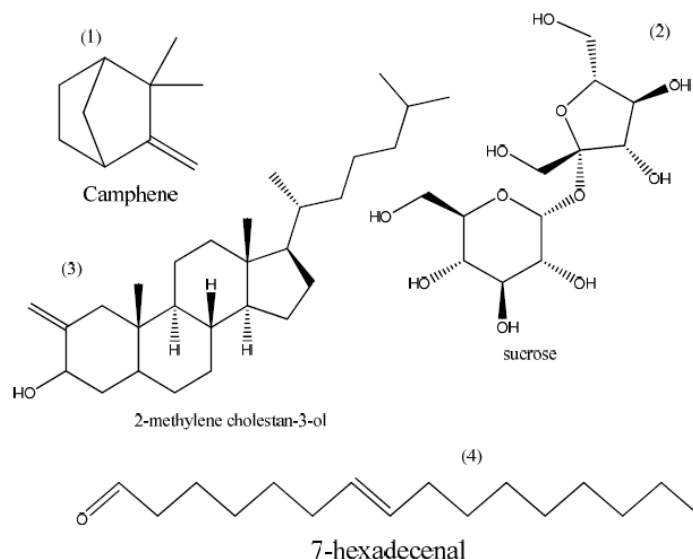


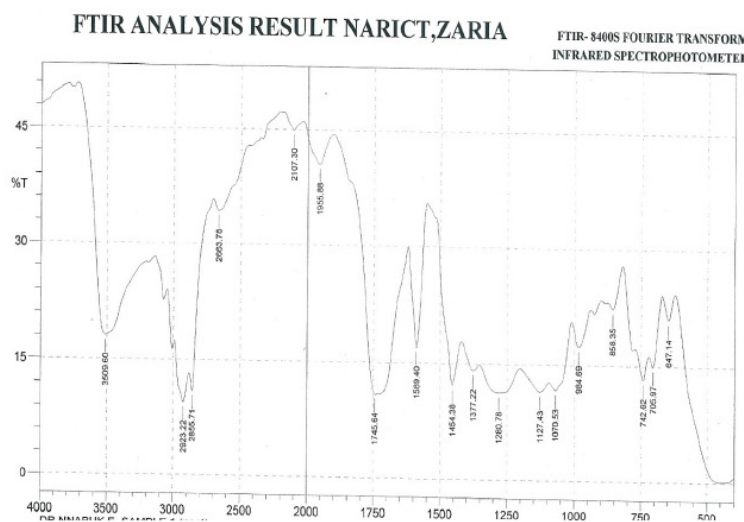
Figure 2. GCMS spectrum of FT gum.

Table 2. Characteristics of the suggested compounds identified from GC-MS gum.

Line No	C(%)	Name of compound	Chemical formula	RT (minute)	Molar mass (g/mol)	Fragmentation peaks
1	4.75	camphene	C <sub>10</sub> H <sub>16</sub>	6.1	136	29(20%), 42(60%), 53(15%), 69(40%), 77(30%), 93(100%), 105(2%),121(15%),134 (15 %).
2	56.15	sucrose	C <sub>12</sub> H <sub>22</sub> O <sub>11</sub>	6.4	342	29(20%), 41(100%), 53(20%), 69(80%), 77(25%), 93(100%), 107(8%), 121(10%), 136(5 %).
3	32.10	2-methylene cholestan-3-ol	C <sub>28</sub> H <sub>48</sub> O	34.0	400	55(50%),71(30%),88(100%0, 101(90%0, 396(30%)
4	7.00	7-hexadecenal	C <sub>16</sub> H <sub>30</sub> O	36.2	238	53(80%), 65(70%), 79(65%), 91(100%),105(80%), 119(90%)



**Figure 3.** Chemical structures of the constituents of FT gum.



**Figure 4.** FTIR spectrum of FT gum.

### FTIR

Fig. 4 presents the FTIR spectrum of FT gum, while frequencies and peaks of IR adsorption by FT gum are presented in Table 3. A close examination of the spectra shows that there are various peaks to the right of  $300\text{ cm}^{-1}$  indicating the presence of alkyl groups (in most organic compounds). A peak was also found to the left of  $300\text{ cm}^{-1}$ . This may be attributed to C=C bond due to camphene or 7-hexadecenal. The presence of sucrose in FT gum is correlated with the presence of cyclopentanone at  $1745\text{ cm}^{-1}$  and several OH vibrations. OH stretch due to alcohol was also found at  $3509.60\text{ cm}^{-1}$ . This may be due to the presence of 2-methylen cholestan-3-ol in the gum. C-H stretches due to alkanes were also found at  $2856$  and  $2923\text{ cm}^{-1}$ . Also at  $1589\text{ cm}^{-1}$ , C-C stretch due to ring was also significant in the spectrum. At peak frequencies of  $1454.38$  and  $1377.22\text{ cm}^{-1}$ , C-H bend and C-H rock due to alkanes were observed. Several C-O vibrations were also found between the wave number range of  $1071$  to  $1281\text{ cm}^{-1}$ . Finally,

between the wave number range of 647 and 985  $\text{cm}^{-1}$ , C-H bend, C-H rock and C-H out of plane vibrations were eminent.

**Table 3.** Peaks and intensity of adsorption of FTIR by *Ficus tricopoda* gum.

Peak ( $\text{cm}^{-1}$ )	Intensity	Area ( $\text{cm}^2$ )	Assignment (functional group)
647.14	21.016	31.693	C-H bend due to alkene
705.97	14.986	37.928	C-H rock due to alkanes
742.62	13.273	42.598	C-H rock due to alkanes
858.35	22.36	34.492	C-H oop due to aromatics
984.69	17.41	51.014	C-H bend due to alkene
1070.53	11.776	71.187	C-O stretch due to alcohol
1127.43	11.544	96.06	C-O stretch due to alcohol
1280.78	11.332	138.509	C-O stretch due to alcohol
1377.22	14.179	36.366	C-H rock due to alkanes
1454.38	12.191	70.73	C-H bend due to alkanes
1589.4	17.016	42.841	C-C stretch in ring
1745.64	10.911	83.487	C=O stretch due to cyclopentanone
2663.78	34.27	112.163	OH stretch due to carboxylic acid
2855.71	10.923	108.588	C-H stretch due to alkanes
2923.22	9.463	102.024	C-H stretch due to alkanes
3509.6	18.049	109.697	OH stretch due to alcohol or phenol

### Corrosion study

#### Effect of FT gum on the corrosion of aluminum

Fig. 5 shows plots for the variation of weight loss with time for the corrosion of Al in 0.1 M of HCl containing various concentrations of FT gum at 303 and 333 K. From the plots, it was deduced that weight loss of Al increases with increase in the period of contact but decreases with increasing concentration of FT gum. These imply that FT gum retarded the corrosion of Al in solution of HCl and that FT gum is an adsorption inhibitor for the corrosion of Al.

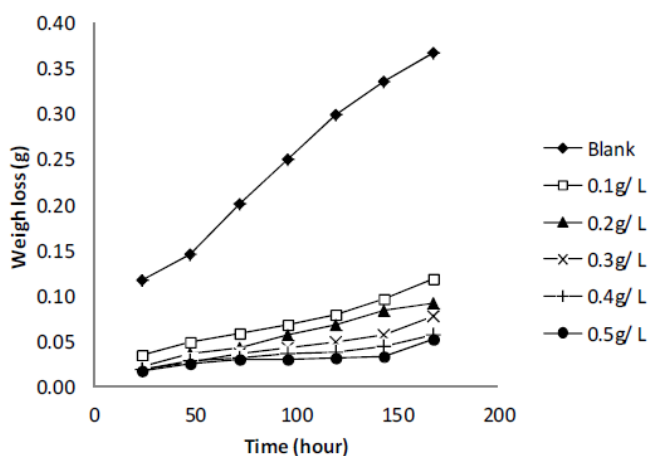


**Figure 5.** Variation of weight loss with time for the corrosion of Al in HCl containing various concentrations of FT gum at 303 K.

Weight loss of Al was also found to decrease with increase in temperature which also suggests that the corrosion rate of Al in solutions of HCl containing FT gum decreases with increase in temperature. In view of the observed trend, values of corrosion rate of Al and inhibition efficiency of various concentrations of FT gum at 303 and 333 K were calculated and are recorded in Table 4. The results

obtained revealed that the inhibition efficiency of FT gum increases with increasing concentration and with increase in temperature at FT gum concentrations above 0.3 g/L. Based on literature, it can be inferred from the pattern of variation of inhibition efficiency with temperature, that two mechanisms of adsorption are possible. A physical adsorption mechanism applied when the inhibition efficiency decreases with increase in temperature, while a chemical adsorption mechanism applied when the inhibition efficiency decreases with increase in temperature [8]. From the calculated values of inhibition efficiency, it can be seen that the mechanisms of physical and chemical adsorption are clearly indicative at lower and higher concentrations of the inhibitors. Hence the mechanism of adsorption of FT gum on Al surface is concentration and temperature dependent.

**Table 4.** Corrosion rates for Al, and inhibition efficiency and degree of surface coverage of FT gum in 0.1 M H<sub>2</sub>SO<sub>4</sub>.

C (g/L)	CR (g/cm <sup>2</sup> /h) at 303 K	%I (303 K)	θ (303 K)	CR (g/cm <sup>2</sup> /h) at 333 K	%I (333 K)	θ (333 K)
Blank	1.63 x 10 <sup>-4</sup>			1.09 x 10 <sup>-4</sup>		
0.1	3.99 x 10 <sup>-5</sup>	75.53	0.7553	3.54 x 10 <sup>-5</sup>	67.51	0.6751
0.2	3.66 x 10 <sup>-5</sup>	77.54	0.7754	2.74 x 10 <sup>-5</sup>	74.88	0.7488
0.3	3.24 x 10 <sup>-5</sup>	80.10	0.8010	2.29 x 10 <sup>-5</sup>	78.98	0.7898
0.4	2.74 x 10 <sup>-5</sup>	83.20	0.8320	1.67 x 10 <sup>-5</sup>	84.71	0.8471
0.5	2.41 x 10 <sup>-5</sup>	85.21	0.8521	1.55 x 10 <sup>-5</sup>	85.80	0.8580

*Kinetic study*

Corrosion of most metals including aluminum has been confirmed to be a first order reaction [22]. Hence the rate of corrosion can be represented as follows [23],

$$-\frac{d[Al]}{[Al]} = k_1 dt \tag{4}$$

where [Al] is the concentration of Al, k<sub>1</sub> is the first order rate constant and t is the time or period of contact. Assuming the concentration of Al at time, t = 0 is denoted as [Al]<sub>0</sub> at time, t = 0 and at some other time, 't' as [Al]. Also, if x g of Al have reacted after time, t, then the concentration of Al at this time will be given as ([Al] – x). Integration of equation 4 within the limit, [Al]<sub>0</sub> and ([Al] – x) yields equation 5 and upon simplification, equations 6 and 7 were obtained

$$-\log\left(\frac{[Al]_0 - x}{[Al]_0}\right) = \frac{k_1 t}{2.303} \tag{5}$$

$$-\log ([Al]_0 - x) = k_1 t/2.303 - \log[Al]_0 \tag{6}$$

$$-\log (\text{weight loss}) = k_1 t/2.303 - \log[Al]_0 \tag{7}$$

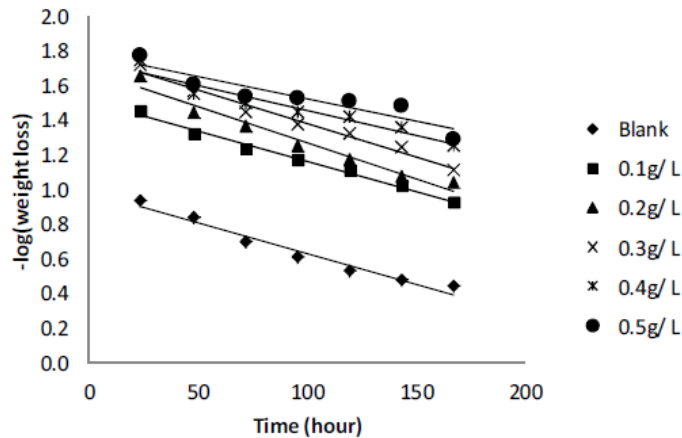


**Figure 6.** Variation of  $-\log(\text{weight loss})$  with time for the corrosion of Al in 0.1 M HCl containing various concentrations of FT gum at 303 K.

**Table 5.** Kinetic parameters for the corrosion of Al in 0.1 M HCl containing various concentrations of FT gum.

T (K)	C (g/L)	slope	intercept	$k_1$	$R^2$	$t_{1/2}$ (hour)
303 K	Blank	0.0036	0.9860	0.0083	1	0.9634
	0.1	0.0035	1.5086	0.0081	2	0.9883
	0.2	0.0042	1.6854	0.0097	2	0.9612
	0.3	0.0039	1.7691	0.0090	2	0.9752
	0.4	0.0029	1.7444	0.0067	2	0.9231
	0.5	0.0026	1.7751	0.0060	2	0.8451
333 K	Blank	0.0028	0.6843	0.0064	1	0.9377
	0.1	0.0031	1.3790	0.0071	2	0.9718
	0.2	0.0030	1.3945	0.0069	2	0.9534
	0.3	0.0028	1.3919	0.0064	2	0.9080
	0.4	0.0021	1.4304	0.0048	2	0.9069
	0.5	0.0020	1.4659	0.0046	3	0.9403

From equation 7, a plot of  $-\log(\text{weight loss})$  versus time should be a straight line with slope and intercept equal to  $k_1/2.303$  and  $\log[\text{Al}]_0$ , respectively. Fig. 6 presents plots for the variation of  $-\log(\text{weight loss})$  versus time for the corrosion of Al in solutions of HCl (plots obtained at 333 K are not shown). Values of  $R^2$ , slopes and  $k_1$  deduced from the plots are presented in Table 5. The half-life of a first order reaction ( $t_{1/2}$ ) is related to the rate constant according to the following equation [22],

$$t_{\frac{1}{2}} = \frac{0.6930}{k_1} \quad (8)$$

From the results obtained (Table 5), it is evident that the half-life for the inhibited reactions of Al in solutions of HCl is higher than those obtained for the blank indicating that FT gum has the tendency to increase the half-life of aluminum in solutions of HCl.

*Effect of temperature*

Effect of temperature on the adsorption of FT gum on mild steel was studied using the logarithm form of the Arrhenius equation (Equation 8) [24]

$$\log \frac{CR_2}{CR_1} = \frac{E_a}{2.303R} \left( \frac{1}{T_1} - \frac{1}{T_2} \right) \quad (9)$$

where  $CR_1$  and  $CR_2$  are the corrosion rates of aluminum in solution of HCl at the temperatures,  $T_1$ (303 K) and  $T_2$  (333 K), respectively,  $E_a$  is the activation energy for the adsorption of FT gum on Al gum and R is the gas constant. Calculated values of the  $E_a$  are shown in Table 6. The activation energies are within the range of values expected for the mechanism of physical adsorption and tend to increase with increase in the concentration of FT gum. This implies that the mechanism of inhibition of Al corrosion by FT gum is concentration dependent. It is also significant to note that the activation energy calculated for the blank is higher than those calculated at FT gum concentrations of 0.1 to 0.3 g/L and vice versa. This implies that less energy is needed for the adsorption of the inhibitor compared to the corrosion of the metal. On the other hand, above FT gum concentration of 0.3 g/L, calculated values of the activation energy were higher than the corresponding value for the blank but lower than the threshold value required for chemisorption. This suggests that at this concentration, the diffusion of the inhibitor's molecules (and not the energy of activation) may be the rate limiting process.

**Table 6.** Activation energy and heat of adsorption of various concentrations of FT gum on Al surface.

C (g/L)	$E_a$ (kJ/mol)	$Q_{ads}$ (kJ/mol)
Blank	11.22	
0.1	3.32	8.31
0.2	8.13	3.08
0.3	9.73	1.45
0.4	13.90	-2.35
0.5	12.41	-1.00

*Thermodynamics and adsorption considerations*

Adsorption of FT gum on Al surface can be exothermic or endothermic depending on the reaction condition, the nature of FT gum's molecules and the mechanism of reaction. In order to calculate the heat of adsorption of FT gum on Al surface, an established thermodynamic equation was used [25]:

$$Q_{ads} = 2.303R \left( \frac{\theta_2}{1-\theta_2} - \frac{\theta_1}{1-\theta_1} \right) \times \left( \frac{T_1 \times T_2}{T_2 - T_1} \right) \quad (10)$$

where  $Q_{ads}$  is the heat of adsorption of FT gum on Al surface,  $\theta_1$  and  $\theta_2$  are the degrees of surface coverage of the inhibitor at the temperatures,  $T_1$  and  $T_2$  (where  $T_2 > T_1$ ) and R is the gas constant. Calculated values of  $Q_{ads}$  (Table 6) reflected endothermic reaction at FT gum concentrations of 0.1 to 0.3 g/L, but an exothermic one at concentrations above 0.3 g/L. This suggests that, above a

critical concentration of 0.3 g/L, the mechanism of inhibition of Al corrosion by FT gum is altered between physisorption to chemisorption.

The adsorption characteristics of an organic corrosion inhibitor can be studied using the adsorption isotherm, whose general form can be written as follows [26],

$$f(\theta, x) \exp(-2a\theta) = bC \quad (11)$$

where  $f(\theta, x)$  is the configurational factor which depends upon the physical model and the assumptions underlying the derivation of the isotherm,  $\theta$ , the surface coverage,  $C$ , the inhibitor concentration in the electrolyte, 'x' is the size factor ratio, 'a' is the molecular interaction parameter and 'b' is the equilibrium constant of the adsorption process. In this study, calculated values of  $\theta$  at various concentrations of the inhibitor were fitted into various adsorption isotherms including Langmuir, Temkin, Freundlich, Flory-Huggins, Bockris-Swinkels and Frumkin isotherms. The test indicated that the adsorption of FT gum best fitted the Langmuir and Frumkin adsorption isotherms.

The Langmuir adsorption isotherm relates the degree of surface coverage to the concentration of the inhibitor according to the following equation [27],

$$\theta = \frac{bC}{(1 + bC)} \quad (12)$$

where  $\theta$  is the degree of surface coverage of the inhibitor,  $C$  is the concentration of the inhibitor in the bulk electrolyte and  $b$  is the adsorption equilibrium constant. Simplification of equation 11 yields equation 12 and from the logarithm of both sides of equation 12, equation 13 was obtained

$$\theta + \theta bC = bC \quad (13)$$

$$\log\left(\frac{C}{\theta}\right) = \log C - \log b \quad (14)$$

Plots of  $\log\left(\frac{C}{\theta}\right)$  versus  $\log b$  gave straight lines and values of  $\log b$  were estimated from intercepts of the plots (Fig.7). Also values of  $R^2$  were very close to unity but slope values were not equal to unity as expected in the Langmuir model indicating the existence of interaction between the inhibitor's molecules.

In order to account for the existence of molecular interaction, the Frumkin adsorption model was found to be applicable to the adsorption of FT gum on Al surface. The Frumkin adsorption isotherm can be expressed as follows [28],

$$\log\left(\frac{\theta}{1-\theta}\right)[C] = \log K + 2a\theta \quad (15)$$

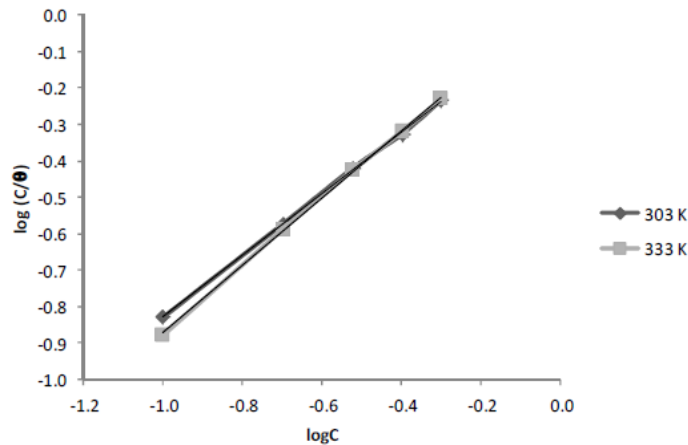


**Figure 7.** Langmuir isotherm for the adsorption of FT gum on Al surface.

From equation 14, a plot of  $\left(\frac{\theta}{1-\theta}\right) [C]$  versus  $\theta$  should be linear if Frumkin isotherm is obeyed. Fig. 8 shows the Frumkin isotherm for the adsorption of FT gum on Al surface. Frumkin adsorption parameters were also deduced from the plots and are presented in Table 7. The results indicated that the interaction parameters are positive and tend to increase with increase in temperature, signifying the attractive behavior of the inhibitor and the possibility of chemisorption mechanism. The adsorption of FT gum on Al surface was also found to be consistent with the Dubinin-Radushkevich (D-RIM) adsorption isotherm, which can be expressed according to equation 12 [29],

$$\ln(\theta) = \ln(\theta_{\max}) - a\sigma^2 \tag{16}$$

where  $\theta_{\max}$  is the maximum surface coverage and  $\sigma$  is the polanyi potential and can be estimated from the following equation,

$$\sigma = RT \ln\left(1 + \frac{1}{C}\right) \tag{17}$$

Straight lines were obtained from plots of  $\ln(\theta)$  versus  $\sigma^2$  indicating the application of the D-RIM isotherm to the adsorption of FT gum on Al surface.

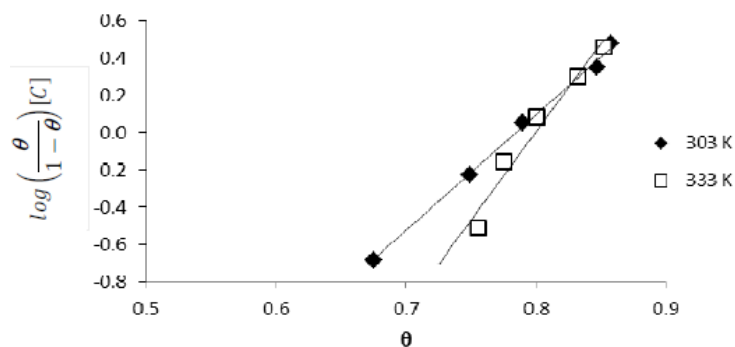


**Figure 8.** Frumkin isotherm for the adsorption of FT gum on Al surface.

The constant ‘a’ and  $\theta_{max}$  were estimated from the slope and intercept of the plot, respectively. The results obtained revealed that the value of ‘a’ at 303 K (i.e.,  $4 \times 10^{-9}$ ) is higher than the value at 333 K ( $7 \times 10^{-9}$ ). Similar trend was observed for values of  $\theta_{max}$  at 303 K (66.64) and 333 K (63.38), respectively. It has been found that the constant, ‘a’ is related to the mean adsorption energy (E) according to equation 17 [29]

$$E = \frac{1}{\sqrt{2a}} \tag{18}$$

**Table 7.** Langmuir and Frumkin parameters for the adsorption of FT gum on Al surface.

Isotherm	T (K)	slope	Intercept	a	R <sup>2</sup>	$\Delta G_{ads}^0$ ( $\frac{kJ}{mol}$ )
Langmuir	303	0.8462	0.0176		0.9997	-10.20
	333	0.9249	0.0517		0.9995	-11.42
Frumkin	303	6.1905	4.8577	3.0953	0.9968	-18.09
	333	9.4993	7.5962	4.7497	0.9672	-37.34

Also, several studies have shown that E value less than 8 kJ/mol supports the mechanism of physical adsorption but E values greater than 8 kJ/mol are consistent with the mechanism of chemisorption. Fig. 9 shows D-RIM isotherm for the adsorption of FT gum on Al surface. R<sup>2</sup> values for the plots were 0.8450 and 0.9636, while E values were 11.18 and 8.55 kJ/mol. From the calculated results, chemisorption mechanism is significant in the inhibition of the corrosion of Al by FT gum.

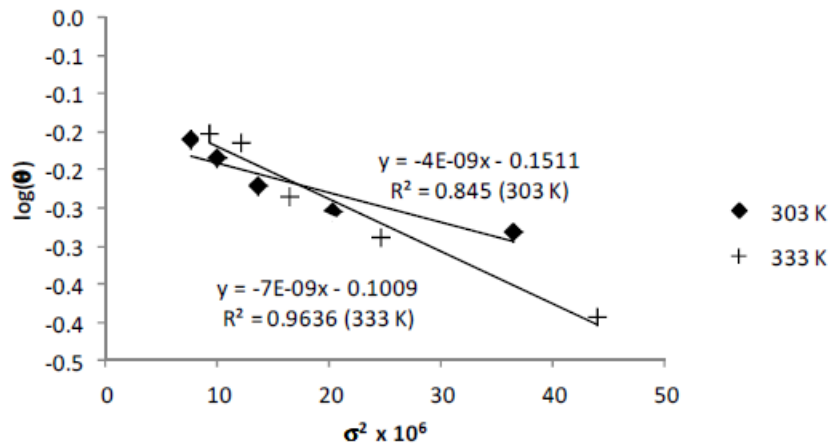


**Figure 9.** D-RIM isotherm for the adsorption of FT gum on Al surface.

The free energy of adsorption of FT gum on Al surface was estimated using the Gibb-Helmoltz equation, which relates the adsorption equilibrium constant with the free energy of adsorption as follows [30 – 31],

$$b = \frac{1}{55.55} \exp\left(\frac{\Delta G_{ads}^0}{RT}\right) \tag{19}$$

where  $\Delta G_{ads}^0$  is the standard free energy of adsorption of FT gum on Al surface. Calculated values of  $\Delta G_{ads}^0$  and 'b' deduced from Langmuir and Frumkin isotherms are presented in Table 7. From the results obtained, the free energies are negative, indicating that the adsorption of FT gum on mild steel surface is spontaneous. However, while free energy values obtained from the Langmuir isotherm point towards a physisorption mechanism, those from the Frumkin isotherm reflect chemisorption mechanism. Hence the adsorption of FT gum is characterized by the initial mechanism of physical adsorption and is succeeded by chemical adsorption mechanism. Generally, values of  $\Delta G_{ads}^0$  below  $-20$  kJ/mol are consistent with the mechanism of charge transfer from the charged inhibitor to the charged metal surface, which supports physisorption, but  $\Delta G_{ads}^0$  values close to or above  $-20$  kJ/mol are consistent with the mechanism of chemical adsorption, which involves the transfer of electrons from the inhibitor's molecules to vacant d-orbital of the metal. From the present data, it is evident that the adsorption of FT gum on Al surface incorporated both mechanisms.

### Conclusions

The results and findings of this study revealed that FT gum is a good inhibitor for the corrosion of Al in solution of HCl. The inhibition potential of the gum is concentration and temperature dependent.

The adsorption of the gum is first order and is characterized by interchanging mechanism. Langmuir, Frumkin and Dubinin-Radushkevich adsorption isotherms are significant in describing the adsorption characteristics of the inhibitors.

In view of the above, the use of FT gum as an inhibitor for the corrosion of Al in acidic medium is hereby recommended.

### References

1. El-Etre AY. Corros Sci. 2003;45:2485.
2. Bouklah M, Hammouti B. Port Electrochim Acta. 2006;24:457.
3. Singh DDN, Singh MM, Chaudhary RS, Agarwal CV. Electrochim Acta 1981;26:1051–1056.
4. Mears RB, Eldredge GG. Ind Eng Chem. 1945;37:736.
5. Singh DDN, Chaudhary RS, Prakash B, Agrawal CV. Br Corros J. 1979;14:235.
6. Metikos-Hukovic M, Babic R, Grubac Z. J Appl Electrochem. 1998;28:433.
7. Amin M, Khaled KF, Mohsen Q, Arida A. Corros Sci. 2010;52:1684.
8. Ramananda SM, Sharma V, Singh G. Port Electrochim Acta. 2011;29:405.
9. Oguzie EE, Onuchukwu AI, Okafor PC, Ebenso EE. Pigment Resin Tech. 2006;35:63.
10. A.M. Abdel-Gaber, B.A. Abd-El-Nabey, I.M. Sidahmed, et al. Corros Sci. 2006;48:2765.
11. Loto CA. Corros. Prev Control. 2001;48:38.
12. El-Etre AY. J Colloid Interf Sci. 2007;314:578.

13. Loto CA. *Corros. Prev Control.* 2003;50:43.
14. El-Etre AY. *Appl Surf Sci.* 2006;252:8521.
15. Umoren SA, Obot IB, Ebenso EE, Egbedi NO. *Port Electrochim Acta* 2008;26:199.
16. Eddy NO, Odiongenyi AO, Ameh PO, Ebenso EE. *Int J Electrochem Sci.* 2012;7:7425.
17. Eddy NO, Ameh PO, Gimba CE, Ebenso EE. *Int J Electrochem Sci.* 2011;6:5677.
18. Eddy NO, Ameh PO, Gimba CE, Ebenso EE. *Int J Electrochem Sci.* 2011;6:5815.
19. Dehri I, Ozcan M. *Mater Chem Phys.* 2006;98:316.
20. Ameh PO, Eddy NO, Gimba CE. *Physiochemical and rheological studies on some natural polymers and their potentials as corrosion inhibitors.* UK: Lambert Academic Publishing; 2012.
21. Carter SJ. *Tutorial pharmacy: solution.* Great Britain: Pitman Press; 2005.
22. Awe FE, Eddy NO. *Amino acids as corrosion inhibitors: quantum and experimental studies.* London, UK: Lambert Academic publishing; 2012.
23. Khaled KF. *Corros Sci.* 2010;52:2905.
24. Okafor PC, Ekpe UJ, Ebenso EE, et al. *Bull Electrochem.* 2005;21:347.
25. Elayyachy M, Hammouti B, El Idrissi A. *Appl Surf Sci.* 2005;249:176.
26. Morad MS, Kamal AM, El-Dean. *Corros Sci.* 2006;48:3398.
27. Behpour M, Ghoreishi SM, Khayatkashani M, Soltani N. *Corros Sci.* 2001;53:2489.
28. Gojic M. *Corros Sci.* 2002;43:919.
29. Noor EA. *J Appl Electrochem.* 2009;39:1465.
30. Dehri I, Ozcan M. *Mater Chem Phys.* 2006;98:316.
31. Popova A, Sokolova E, Raicheva S, Christov M. *Corros Sci.* 2003;45:33.